

# Influence of poly(ethylene glycol)/montmorillonite hybrids on the rheological behaviors and mechanical properties of polypropylene

Shipeng Zhu · Jinyao Chen · Huilin Li

Received: 14 January 2009 / Revised: 24 March 2009 / Accepted: 15 April 2009 /  
Published online: 26 April 2009  
© Springer-Verlag 2009

**Abstract** The effects of poly(ethylene glycol) (PEG)/montmorillonite (MMT) hybrids on the phase morphology, rheological behaviors and mechanical properties of polypropylene (PP) were investigated. The analysis of transmission electron microscopy (TEM) and wide-angle X-ray diffraction (WAXD) indicated that the PEG modified montmorillonite was intercalated and well dispersed into PP matrix. It was found that the addition of the PEG/MMT hybrids in PP matrix lead to a significant reduction of melt viscosity and enhancement in izod-notched impact strength and elongation at break, except that the tensile strength was without much obvious change. A quantitative analysis indicated that MMT was intercalated by PEG, which was responsible for the melt viscosity reduction of PP matrix. Differential scanning calorimetry (DSC) analysis indicated that the addition of PEG/MMT hybrids induced the formation of  $\beta$ -crystal of PP. Polarized light micrographs (PLM) analysis indicated that the dispersed MMT, which acted as a nucleating agent, lowered the spherulite dimension and increased the spherulite number, resulting in high izod-notched impact strength and elongation at break.

**Keywords** Polypropylene · Montmorillonite · Rheological behaviors · Mechanical properties

## Introduction

Polypropylene (PP), one of the most important thermoplastic, is widely used in industry due to its well balanced properties and low price. However, its correspondingly poor impact strength restricts its application in automobile and

---

S. Zhu · J. Chen · H. Li (✉)  
State Key Laboratory of Polymer Materials Engineering, Polymer Research Institute of Sichuan University, 610065 Chengdu, Sichuan, People's Republic of China  
e-mail: nic7703@scu.edu.cn

package fields as substitute for high performance engineering plastic [1, 2]. In order to overcome its disadvantages, a great deal of work has been done in the past several decades. The introduction of montmorillonite (MMT) is an effective way to improve the properties of PP [3–8]. However, it is very difficult to obtain PP/MMT nanocomposites because MMT is incompatible with PP which does not include any polar groups in its backbone [9]. Kawasumi et al. [10] first succeeded in preparing PP/MMT nanocomposites in presence of a maleic anhydride modified polypropylene oligomer compatibilizer.

It is well known that the excellent properties of polymer/clay nanocomposites derive from the improvement of interfacial properties and unique phase morphology. There are two ideal types of nanostructures in PP/MMT nanocomposites, intercalation and exfoliation. When a few polymer molecules are inserted into the MMT gallery, the intercalated structure is formed due to the increase of the interlayer spacing. Exfoliated structure is formed when the silicate layers are individually dispersed in PP matrix. Real morphologies of PP/MMT nanocomposites often fall in between the two idealized microstructures [11, 12]. Although all these structures often coexist in the PP/MMT nanocomposites, it is believed that the remarkable mechanical, flammability and barrier properties of these materials derive from the large amount of the exfoliated nanometer silicate layers [13–20].

Recently, the relationships between the melt rheological behaviors and structures of polymer/layered silicate nanocomposites have been intensively studied [21, 22]. Many unusual rheological phenomena of polymer nanocomposites have been reported [23–25]. Our previous investigation indicated that poly(ethylene glycol)(PEG)/organophilic montmorillonite (OMMT) hybrids and polypropylene in ultrahigh molecular weight polyethylene (UHMWPE) matrixes could lead to a significant reduction of melt viscosity and improve mechanical properties of UHMWPE [26]. According to the studies of Aranda and Ruiz-Hitzky [27] and Greeland [28], polymers which contain the groups capable of associative interactions, such as hydrogen bonding, lead to intercalation. The strong hydrogen bonding between the oxygen groups of PEG and hydroxyl groups from OMMT drives the intercalation. The intercalated PEG chains improve the interaction of OMMT and UHMWPE, producing the intercalated and exfoliated OMMT in the matrix [29].

In this paper, PP/MMT nanocomposites were prepared through melt blending, and the effects of PEG/MMT hybrids on the rheological behaviors and mechanical properties of PP were investigated, aiming at relating the rheological behaviors and mechanical properties of the PP/MMT nanocomposites with phase morphologies. The possible mechanisms of enhancement in mechanical properties and reduction of melt viscosity have been proposed.

## Experimental

### Materials

Poly(ethylene glycol) (PEG) was supplied by Liaoyang Aoke Chemical Co. (Liaoning, China) with a molecular weight of 6000. Polypropylene (PP) (F401)

was supplied from Langang Chemical Industry Factory (Lanzhou, China). Na<sup>+</sup>-montmorillonite (Na<sup>+</sup>-MMT) with a cation-exchange capacity (CEC) of 90 mmol/100 g and Organophilic montmorillonite (OMMT) named DK-1 was supplied by Zhejiang Fenghong Clay Chemicals Co. (Zhejiang, China) with a BET surface area of 150 m<sup>2</sup>/g. DK-1 is a natural montmorillonite modified with hexadecyltrimethylammonium chloride.

### Sample preparation

PEG was first dissolved in ethanol to form a uniform solution. The Na<sup>+</sup>-MMT powder was subsequently added to the uniform solution. The mixture was then heated to 60 °C for 6 h under vigorous stirring and formed a homogeneous suspension. The PEG/Na<sup>+</sup>-MMT (PM) hybrids were dried in a 60 °C oven for several days and then pulverized into 70- $\mu$ -sized particles in a high shear mixer. PEG/OMMT (POM) hybrids were prepared in the same way. The PEG/Na<sup>+</sup>-MMT and PEG/OMMT with weight ratio 1:1, 2:1 were designated as PM11, PM21 and POM11, POM21, respectively. The addition of PM or POM hybrids were 1–7 parts per hundred parts of PP (phr) by weight, then extruded by a general three-section twin-screw extruder ( $D = 20$  mm,  $L/D = 40$ ). Screw speed was set at 200 rpm and the temperatures were 175, 190, and 190 °C for each section of the barrel and 185 °C for the die. An injection-molding machine (K-TEC400, Klarke international Co., Ltd.) was used to prepare the specimens for the mechanical tests.

### Rheological experiments

The rheological measurements were carried out on a Gottfert Rheograph 2002 (Gottfert Co., Germany). The capillary diameter and its length-to-diameter ratio were 1 mm and 30, respectively. The die had an entrance angle of 180 °C. Entrance pressure losses were assumed to be negligible for such a long capillary die, and therefore no Bagley correction was applied. The flow properties of these specimens were measured at 190 °C.

### Mechanical properties

Tensile tests were carried out according to GB/T 1040-92 standard on CMT 4104 machine (Sans Material Testing Technical Co., Shenzhen, China). Elongation at break was measured at a cross-head speed of 50 mm/min. Izod-notched impact strength was measured with ZQK-20 (Dahua Material Testing Technical Co., China) according to GB/T1043-93 standard.

### Wide-angle X-ray diffraction

Wide-angle X-ray diffraction (WAXD) spectra were recorded with a DX-1000 CSC diffractometer (China). The X-ray beam was nickel-filtered Cu Ka ( $\lambda = 0.1542$  nm) radiation operated at 40 kV and 35 mA. Na<sup>+</sup>-MMT, OMMT, PM11 and POM11 were studied as powders. Samples of PP/PM11 and PP/POM11 composites were

from the injection molded. The scanning range was varied from  $2\theta = 2^\circ$  to  $10^\circ$  with a rate of  $1.8^\circ/\text{min}$ .

#### Transmission electron microscopy

Transmission electron microscopy (TEM) observations were carried out with an H-7100 (Tokyo, Japan) instrument with an accelerating voltage of 100 kV. The ultrathin sections of the samples from injection molded with a thickness of 100 nm were microtomed at  $20^\circ\text{C}$  by a Reichert Ultracut cryoultramicrotome without staining.

#### Thermal analysis

Crystallization studies were performed on a DSC1 (Mettler Toledo Co., Switzerland) differential scanning calorimeter under constant nitrogen flow. Sample weight was maintained at low level (4–5 mg) for all measurements. All samples were first heated to  $200^\circ\text{C}$ , held at  $200^\circ\text{C}$  for 5 min, and then cooled with a rate  $10^\circ\text{C}/\text{min}$  to  $50^\circ\text{C}$ , and held at  $50^\circ\text{C}$  for 5 min. They were then scanned from 50 to  $200^\circ\text{C}$  at a rate of  $10^\circ\text{C}/\text{min}$ .

#### Polarizing light microscopy

Polarized light micrographs (PLM) were taken on a Leitz Laborlux 12POL (Leitz Co., Germany) at  $200\times$  magnification. Samples were prepared through cutting small pieces from prepared films. Samples weighing 25 mg were melted on glass slides with cover slips to form thin films with  $25\ \mu\text{m}$  thick.

## Results and discussion

### Rheological behaviors

The effects of PM and POM hybrids on the rheological properties of PP were investigated, as shown in Figs. 1 and 2 and Table 1. All composites exhibit the non-Newtonian and shear thinning behaviors.

Figure 1 shows the influence of different additives on the rheological properties of PP. When  $\text{Na}^+$ -MMT or OMMT powder is directly added into PP matrix, the melt viscosity of the composites reduces a little. However, the addition of PM and POM hybrids reduces the apparent viscosity of PP significantly at shear rates less than  $576\ \text{s}^{-1}$ . The more PM or POM hybrids are added, the more viscosity reduction of PP is occurred. When 7 phr POM21 is added, the apparent viscosity of PP/POM21 composites decreases to 49% at the shear rate of  $115.2\ \text{s}^{-1}$ .

Figure 2 shows the rheological behaviors of different PP/PM and PP/POM composites with the same hybrids content. The comparison of the flow behaviors of PP/PM11 (100/5), PP/POM11 (100/5), PP/PM21 (100/5), and PP/POM21 (100/5) indicates that the weight ratio of PEG/ $\text{Na}^+$ -MMT (or PEG/OMMT) has a significant

*Rheological behaviors*

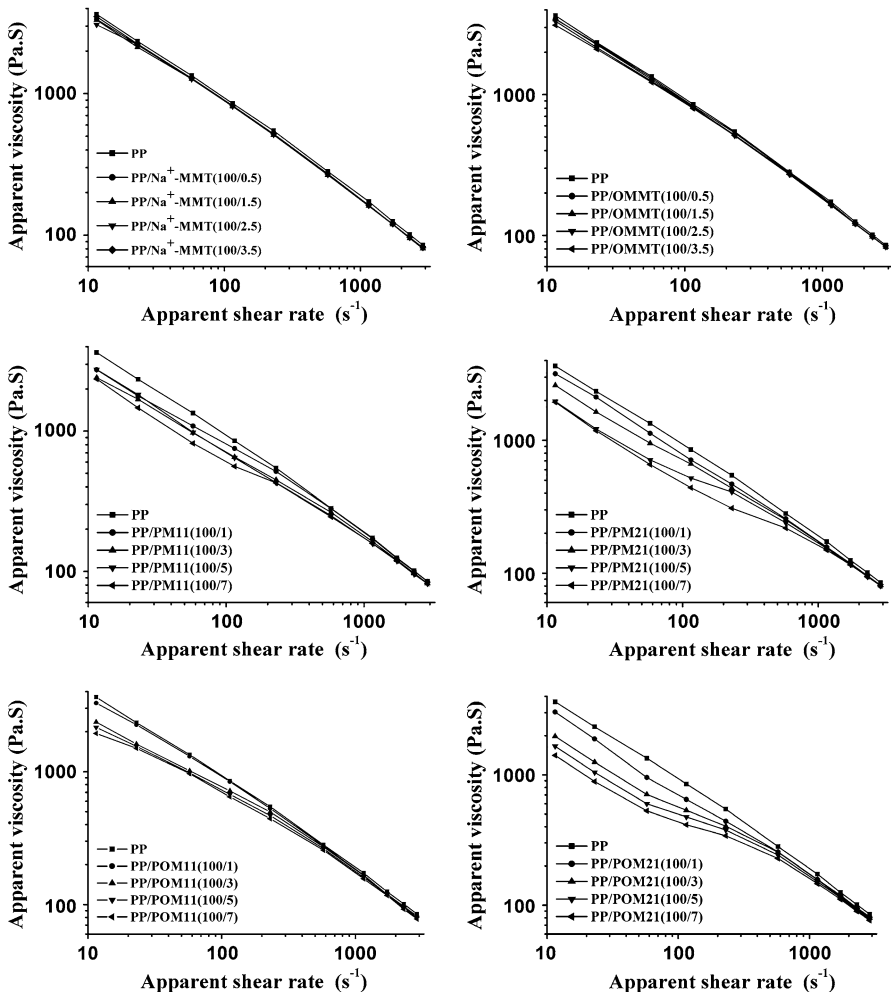


**Fig. 1** Plot of the logarithm of the apparent viscosity versus the logarithm of the apparent shear rate for PP and PP/MMT composites

influence on the viscosity reduction of PP. The PP/PM21 and PP/POM21 composites show more viscosity reduction than PP/PM11 and PP/POM11 composites. In other words, the more PEG was added into Na<sup>+</sup>-MMT or OMMT, the more viscosity reduction of PP occurred. Table 1 shows the relative apparent viscosity of PP/PM and PP/POM composites at different apparent shear rates. With 5 phr POM21 in the PP, the apparent melt viscosity is much lower than that of pure PP and the other PP/MMT composites at shear rates less than 576 s<sup>-1</sup>.

Gai has reported that the interfacial adhesion strength between PEG and PP is only 7.1 mJ/m<sup>2</sup> and PEG molecules still covered on OMMT layers, instead of being replaced by PP or UHMWPE molecules in the extrusion of the UHMWPE/PP/PM

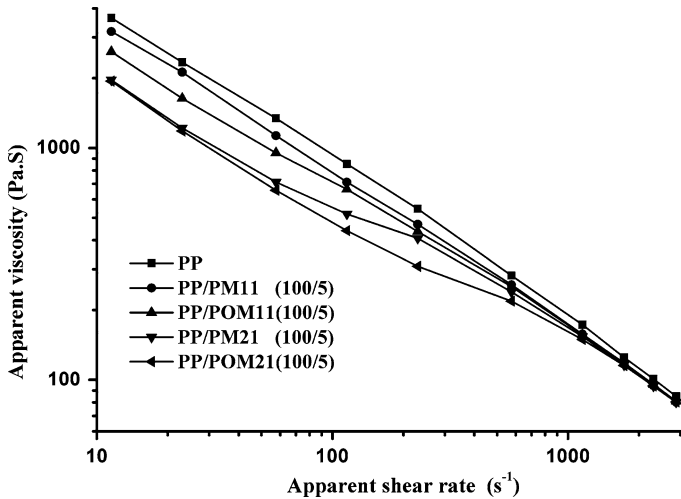


**Fig. 2** Plot of the logarithm of the apparent viscosity versus the logarithm of the apparent shear rate for PP, PP/PM, and PP/POM composites

**Table 1** The relative apparent viscosity of PP/PM and PP/POM nanocomposites at different apparent shear rates

Samples	$57.6 \text{ s}^{-1}$	$115.2 \text{ s}^{-1}$	$230.4 \text{ s}^{-1}$	$576 \text{ s}^{-1}$
PP/PM11(100/5)	84.2%	83.5%	85.8%	91.3%
PP/POM11(100/5)	70.9%	77.8%	79.9%	89.8%
PP/PM21(100/5)	53.1%	60.9%	74.8%	85.1%
PP/POM21(100/5)	48.9%	51.6%	56.6%	77.7%

The apparent viscosity of PP is defined as 1

system [26]. It indicates that PP is incompatible with PEG which has very low viscosity and good lubricating property. The intercalated silicate layers may be used as a lubricant carrier in the composites. In other words, the short PEG chains on the surface of MMT can act as an internal lubricant to induce interphase slippage of the composites. The quantitative relationship between PEG and MMT effect on rheological behaviors and phase morphologies of the PP/MMT nanocomposites needs to be studied further.

### Mechanical properties

Tables 2 and 3 summarize the mechanical properties of PP, PP/PM, and PP/POM composites. The mechanical properties such as elongation at break and izod-notched impact strength are improved. The mechanical properties of PP/POM composites are better than those of PP/PM composites, especially the izod-notched impact strength. The mechanical properties of PP/POM11 composites with 5 phr POM11 are much better than those of other composites. When 5 phr of POM11 is

**Table 2** The mechanical properties of PP and PP/MMT composites

Sample	Tensile strength (MPa)	Elongation at break (%)	Izod-notched impact strength (kJ/m <sup>2</sup> )
PP	31.62	74.46	3.93
PP/Na <sup>+</sup> -MMT(100/0.5)	31.93	64.23	4.14
PP/Na <sup>+</sup> -MMT(100/1.5)	31.61	93.00	4.56
PP/Na <sup>+</sup> -MMT(100/2.5)	31.20	81.15	4.72
PP/Na <sup>+</sup> -MMT(100/3.5)	31.54	66.32	5.25
PP/PM11 (100/1)	30.85	94.20	5.90
PP/PM11 (100/3)	30.52	111.46	6.35
PP/PM11 (100/5)	30.60	81.29	7.05
PP/PM11 (100/7)	30.23	120.79	7.15
PP/PM21 (100/1)	30.63	108.59	6.56
PP/PM21 (100/3)	31.01	91.53	6.62
PP/PM21 (100/5)	30.76	115.69	6.90
PP/PM21 (100/7)	30.80	117.23	7.40

**Table 3** The mechanical properties of PP and PP/OMMT composites

Sample	Tensile strength (MPa)	Elongation at break (%)	Izod-notched impact strength (kJ/m <sup>2</sup> )
PP	31.62	74.46	3.93
PP/OMMT(100/0.5)	32.23	85.82	5.38
PP/OMMT(100/1.5)	31.80	111.84	6.29
PP/OMMT(100/2.5)	31.96	106.73	7.11
PP/OMMT(100/3.5)	32.02	105.51	7.21
PP/POM11 (100/1)	31.51	165.03	6.28
PP/POM11 (100/3)	31.04	207.30	9.67
PP/POM11 (100/5)	30.52	181.13	11.80
PP/POM11 (100/7)	29.90	165.04	12.03
PP/POM21 (100/1)	31.38	143.79	5.91
PP/POM21 (100/3)	31.20	213.40	7.92
PP/POM21 (100/5)	30.70	220.66	9.95
PP/POM21 (100/7)	30.12	163.53	10.69

added, the izod-notched impact strength and elongation at break of PP increase by 200 and 143%, respectively. Additionally, compared with pure PP, the tensile strength of all samples has no obvious change with increasing the content of different additives. It is notable that the mechanical properties of PP/PM composites can compare favorably with PP/OMMT composites.

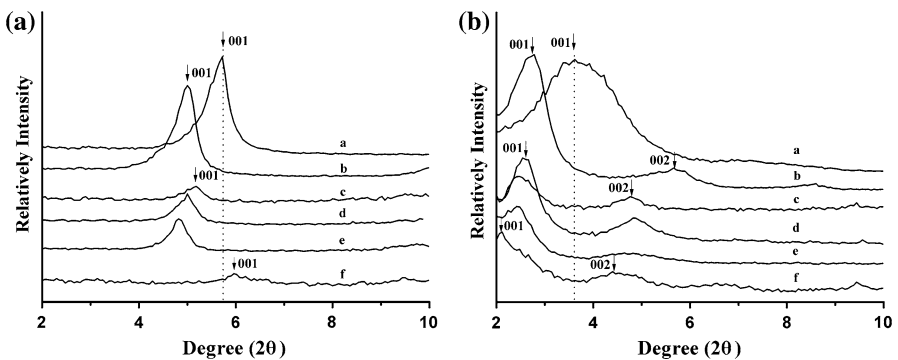
## The dispersion of MMT platelets in the composites

Figure 3 shows the respective X-ray diffraction curves for the various MMT and their Composites. The interlayer spacing of the (001) plane ( $d_{001}$ ) for the  $\text{Na}^+$ -MMT sample estimated by Bragg's formula  $n\lambda = 2d\sin 2\theta$  is 1.55 nm ( $2\theta = 5.71^\circ$ ). The identification of the (001) diffraction peaks is summarized for all investigated samples in Table 4.

As it is shown in Fig. 3A and Table 4, compared with that of the virgin clay power, the (001) diffraction peak for PM11 powder is found to shift, in a comparatively short range, from  $2\theta = 5.71^\circ$  ( $d_{001} = 1.55$  nm) to  $5.00^\circ$  ( $d_{001} = 1.77$  nm). It indicates that PEG has intercalated into the silicate layers. However, the interlayer spacing of silicate layers in PP/PM11 is almost unchanged compared with PM11. It is apparent that in PP/PM11 composites, no PP molecular chains diffused into the interlayer of PM11.

Figure 3B and Table 4 show the interlayer spacing of OMMT is 2.44 nm ( $2\theta = 3.62^\circ$ ). The  $d_{001}$  peak of POM11 increases to 3.18 nm ( $2\theta = 2.78^\circ$ ). This result implies that PEG has intercalated into the silicate layers. The interlayer spacing of silicate layers in PP/POM11 is larger than POM11. These results indicate that PP molecular chains have intercalated into the interlayer of POM11. The interlayer spacing of OMMT in PP/OMMT increase to 4.28 nm ( $2\theta = 2.06^\circ$ ). It is apparent that in PP/OMMT composites, PP molecular chains diffused into the gallery of the clay.

To further confirm the microstructure, TEM of PP/PM11 and PP/POM11 composites were taken. Bright field is the image of polymer, in which dark entities are the cross-section of intercalated silicate layers. As can be seen in Fig. 4a–d, no matter  $\text{Na}^+$ -MMT and PM11, some aggregate of MMT platelets could be found at the image of TEM. It suggested that there existed neither intercalation nor exfoliation structure in the composite. However, the silicate layers of OMMT and POM11 were intercalated in the matrix (Fig. 4e–h). The POM11 hybrids were well dispersed in PP matrix (Fig. 4h). The melt intercalation is controlled by the mass



**Fig. 3** Wide-angle X-ray diffraction patterns. **A** (a)  $\text{Na}^+$ -MMT, (b) PM11, (c) PP/PM11(100/1), (d) PP/PM11(100/3), (e) PP/PM11(100/5), (f) PP/ $\text{Na}^+$ -MMT(100/1.5); **B** (a) OMMT, (b) POM11, (c) PP/POM11(100/1), (d) PP/POM11(100/3), (e) PP/POM11(100/5), (f) PP/OMMT (100/1.5)



**Table 4** (001) Diffraction peaks and corresponding *d*-spacing of various MMT and their composites

Sample	Peak position (°)	<i>d</i> -spacing (nm)
Na <sup>+</sup> -MMT	5.71	1.55
PM11	5.00	1.77
PP/PM11 (100/1)	5.18	1.71
PP/PM11 (100/3)	5.00	1.77
PP/PM11 (100/5)	4.82	1.83
PP/Na <sup>+</sup> -MMT (100/1.5)	6.01	1.47
OMMT	3.62	2.44
POM11	2.78	3.18
PP/POM11 (100/1)	2.54	3.48
PP/POM11 (100/3)	2.54	3.48
PP/POM11 (100/5)	2.42	3.64
PP/OMMT (100/1.5)	2.06	4.28

transport of polymer chain into the primary particles of clay, and tactoids near the edge may be accessible to the polymer chain. Thus it can be inferred that silicate layers at the end of the silicate stacks may be relatively easy to be exfoliated. All the observations from Fig. 4 are well consistent with WAXD results.

The viscosity reduction of PP/POM11 nanocomposites is higher than that of PP/PM11 composites. We have confirmed that the increment of *d*-spacing for POM11 and PM11 are 0.74 and 0.22 nm, respectively. This indicates that more PEG intercalated into the clay layers of POM11 compared with PM11. Adequate intercalation of PEG molecules into the clay layers or coating the layers surface expedites the exfoliation of clay layers in the matrix, followed by the slippage of the clay layers coated with PEG among the matrix and the reduction of the viscosity of the PP matrix. We could also conclude that better dispersion of POM11 compared with PM11 in PP matrix (Fig. 4), which was good for reduction of melt viscosity.

#### Crystal structure and crystallinity

Clay can help to improve the heterocrystallization of polymer/clay nanocomposites, which can induce the formation of  $\beta$ -crystal [30]. Dragaun et al. [31] and Samueles [32] had found that the melting point of  $\beta$ -crystal was from 140 to 153 °C. Figure 5 shows the melting behaviors of PP/PM and PP/POM composites. As it is shown in Fig. 5A, the melting peak of the  $\beta$ -crystal is not observed in the DSC curves of pure PP. However, the melting peak of the  $\beta$ -crystal appears near 145 °C in the PP/PM11 composites. The situation is also discovered in Fig. 5B. The melting peak of  $\beta$ -crystal also appeared near 145 °C in the PP/POM11 composites. These results indicate that the addition of PM or POM hybrids can induce the formation of the  $\beta$ -crystal.

Figure 6 shows the typical spherulitic texture of PP and its composites. The spherulite size gradually decreases with increasing the PM11 and POM11 content.

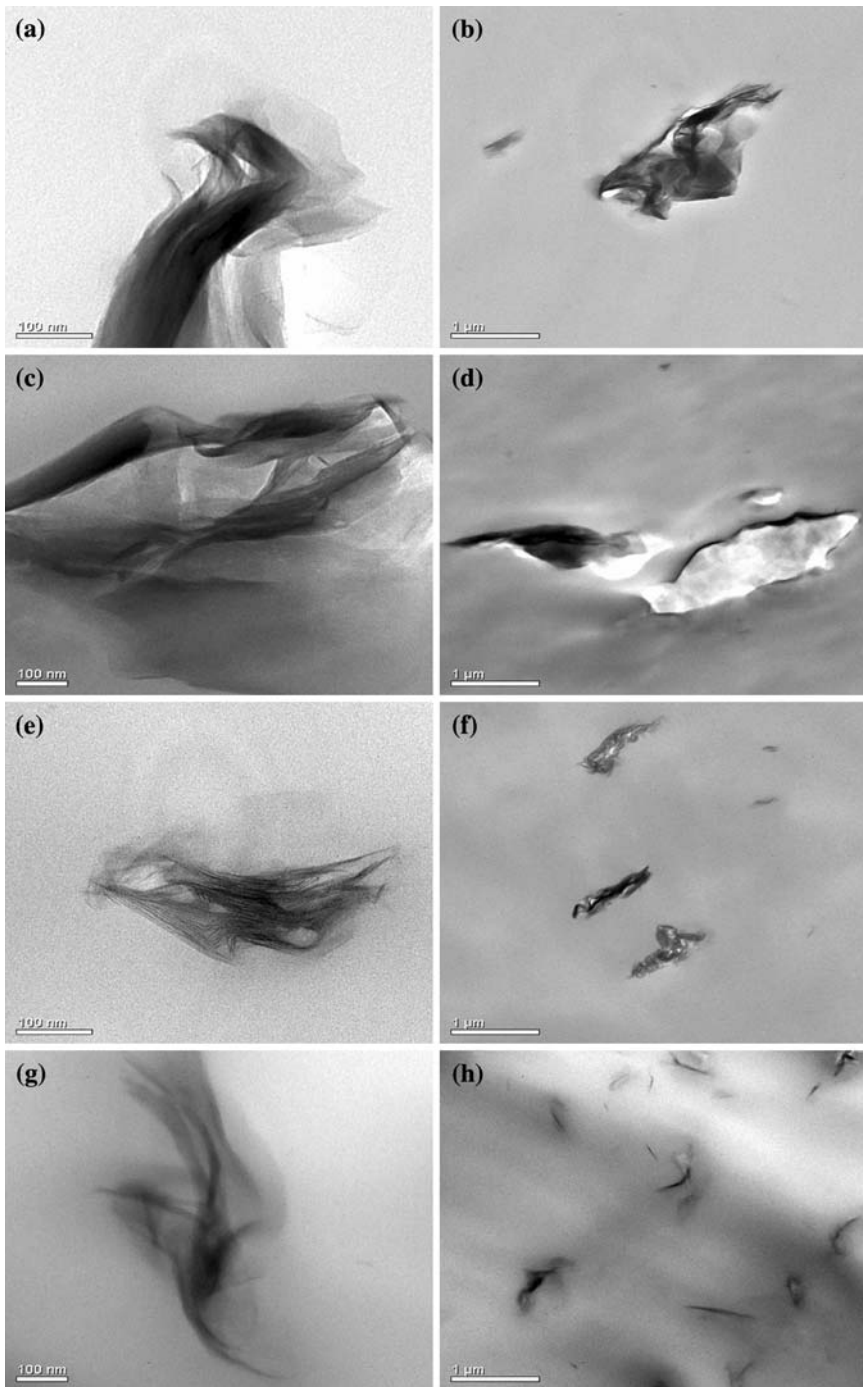


**Fig. 4** Transmission electron micrographs of (a) and (b) PP/ $\text{Na}^+$ -MMT (100/2.5), (c) and (d) PP/PM11 (100/5), (e) and (f) PP/OMMT (100/2.5), (g) and (h) PP/POM11 (100/5)

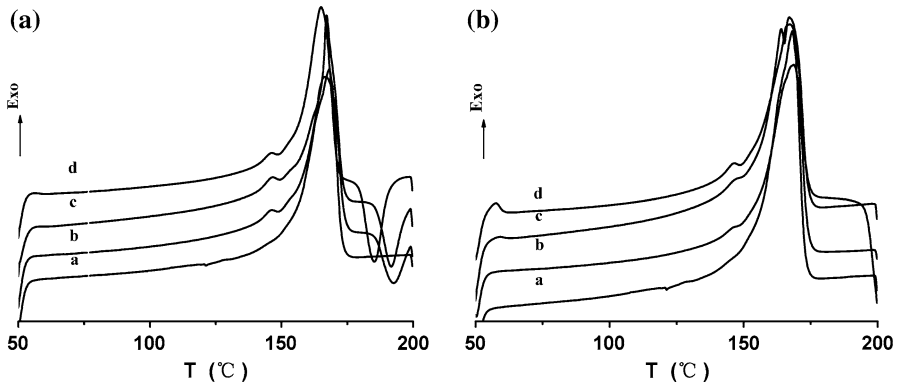


**Fig. 5** DSC curves of **A** (a) PP, (b) PP/PM11 (100/1), (c) PP/PM11 (100/3), (d) PP/PM11 (100/5); **B** (a) PP, (b) PP/POM11 (100/1), (c) PP/POM11 (100/3), (d) PP/POM11 (100/5)

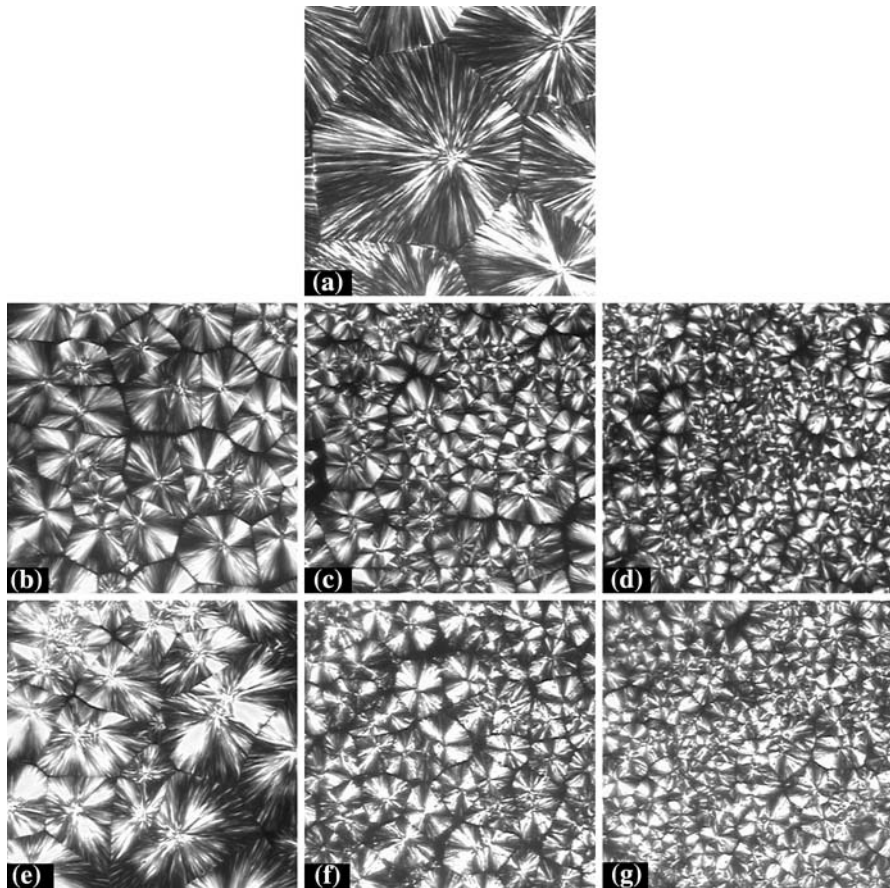


**Fig. 6** Polarization light micrographs of (a) PP, (b) PP/PM11(100/1), (c) PP/PM11(100/3), (d) PP/PM11(100/5), (e) PP/POM11(100/1), (f) PP/POM11(100/3), (g) PP/POM11(100/5).( $\times 200$ )

The dispersed clay particles can act as a nucleating agent, which is proved by the fact that the increase in the number density of nuclei causing the smaller spherulites.

## Conclusions

The effects of PM and POM hybrids on the rheological behaviors and mechanical properties of PP were investigated. The melt viscosity of the composites changed slightly when Na<sup>+</sup>-MMT or OMMT powder was directly added into PP. However, the addition of PM and POM hybrids reduced the apparent viscosity of PP. The addition of a small amount of POM21 could reduce the melt viscosity of PP matrix significantly. The mechanical properties of PP/POM11 composites with 5 phr POM11 were much better than those of other composites.

The WAXD analysis and TEM observation clarified the formation of exfoliated and intercalated structure in the PP/MMT nanocomposites. Unlike PP, PEG could intercalate into the silicate layers of Na<sup>+</sup>-MMT and OMMT. However, PP molecular chains could intercalate into the interlayer of POM11 other than PM11. The POM hybrids were well dispersed in PP matrix. The effect of POM11 on viscosity reduction of PP was better than that of PM11 due to their different dispersion and nanostructure. DSC analysis indicated that the addition of PM and POM hybrids could induce the  $\beta$ -crystal of PP to form. PLM observation indicated that the dispersed MMT, which acted as a nucleating agent, lowered the spherulite dimension and increased the spherulite number.

**Acknowledgment** National Basic Research Program of China (2005CB623800).

## References

1. Manias E, Touny A, Wu L, Strawhecker K, Lu B, Chung TC (2001) Polypropylene/montmorillonite nanocomposites. Review of the synthetic routes and materials properties. *Chem Mater* 13:3516
2. Lin ZH, Peng M, Zheng Q (2004) Isothermal crystallization behavior of polypropylene catalloys. *J Appl Polym Sci* 93:877
3. Gianelli W, Ferrara G, Camino G, Pellegatti G, Rosenthal J, Trombini RC (2005) Effect of matrix features on polypropylene layered silicate nanocomposites. *Polymer* 46:7037
4. Paul MA, Alexandre M, Degee P, Henrist C (2003) New nanocomposite materials based on plasticized poly(L-lactide) and organo-modified montmorillonites: thermal and morphological study. *Polymer* 44:443
5. Michael JS, Abdulwahab S, Almusallam KF (2001) Rheology of polypropylene/clay hybrid materials. *Macromolecules* 34:1864
6. He AH, Wang LM, Li JX, Dong JY, Han CC (2006) Preparation of exfoliated isotactic polypropylene/alkyl-triphenylphosphonium-modified montmorillonite nanocomposites via in situ intercalative polymerization. *Polymer* 47:1767
7. Ding C, He H, Guo BC, Jia DM (2008) Structure and properties of polypropylene/clay nanocomposites compatibilized by solid-phase grafted polypropylene. *Polym Compos* 29:698
8. Zhang Q, Wang Y, Fu Q (2003) Shear-induced change of exfoliation and orientation in polypropylene/montmorillonite nanocomposites. *J Polym Sci Part B Polym Phys* 41:1
9. Shi D, Yu W, Li KY, Ke Z, Yin JH (2007) An investigation on the dispersion of montmorillonite primary particles in PP matrix. *Eur Polym J* 43:3250
10. Kawasumi M, Hasegawa N, Kato M, Usuki A, Okada A (1997) Preparation and mechanical properties of polypropylene-clay hybrids. *Macromolecules* 30:6333

11. Vaia RA, Lincoln D, Wang ZG, Hsiao BS (2000) Crystallization of polymers in confined environments: structural development of semi-crystalline polymer-layered silicate nanocomposites. *Polym Mater Sci Eng* 82:257
12. Hwu JM, Jiang GJ (2005) Preparation and characterization of polypropylene-montmorillonite nanocomposites generated by in situ metallocene catalyst polymerization. *J Appl Polym Sci* 95:1228
13. Tang Y, Hu Y, Wang SF (2003) Intumescent flame retardant-montmorillonite synergism in polypropylene-layered silicate nanocomposites. *Polym Int* 52:1396
14. Gregoriou VG, Kandilioti G, Bolas ST (2005) Chain conformational transformations in syndiotactic polypropylene/layered silicate nanocomposites during mechanical elongation and thermal treatment. *Polymer* 46:11340
15. Chung MJ, Jang LW, Shim JH (2005) Preparation and characterization of maleic anhydride-g-polypropylene/diamine-modified clay nanocomposites. *J Appl Polym Sci* 95:307
16. Hu Y, Tang Y, Song L (2006) Poly (propylene)/clay nanocomposites and their application in flame retardancy. *Polym Adv Technol* 17:235
17. Xu WB, Liang GD, Wang W (2003) PP-PP-g-MAH-Org-MMT nanocomposites. I. Intercalation behavior and microstructure. *J Appl Polym Sci* 88:3225
18. Kim DH, Fasulo PD, Rodgers WR, Paul DR (2007) Structure and properties of polypropylene-based nanocomposites: Effect of PP-g-MA to organoclay ratio. *Polymer* 48:5308
19. Gilman JR, Jackson CL, Morgan BA (2000) Flammability properties of polymer-layered-silicate nanocomposites. Polypropylene and polystyrene nanocomposites. *Chem Mater* 12:1866
20. Dumont MJ, Emond JP, Bousmina M (2007) Barrier properties of polypropylene/organoclay nanocomposites. *J Appl Polym Sci* 103:618
21. Krishnamoorti R, Vaia RA, Giannelis EP (1996) Structure and dynamics of polymer-layered silicate nanocomposites. *Chem Mater* 8:1728
22. Krishnamoorti R, Giannelis EP (1997) Rheology of end-tethered polymer layered silicate nanocomposites. *Macromolecules* 30:4097
23. Li J, Zhou CX, Wang G, Zhao DL (2003) Study on rheological behavior of polypropylene/clay nanocomposites. *J Appl Polym Sci* 89:3609
24. Zhao J, Morgan AB, Harris JD (2005) Rheological characterization of poly styrene-clay nanocomposites to compare the degree of exfoliation and dispersion. *Polymer* 46:8641
25. Sun TC, Chen FH, Dong X, Han CC (2008) Rheological studies on the quasi-quiescent crystallization of polypropylene nanocomposite. *Polymer* 49:2717
26. Gai JG, Li HL (2007) Influence of organophilic montmorillonite and polypropylene on the rheological behaviors and mechanical properties of ultrahigh molecular weight polyethylene. *J Appl Polym Sci* 105:1200
27. Aranda P, Ruiz-Hitzky E (1992) Poly(ethylene oxide)-silicate intercalation materials. *Chem Mater* 4:1395
28. Greeland DJ (1963) Adsorption of poly(vinyl alcohols) by montmorillonite. *J Colloid Sci* 18:647
29. Gai JG, Li HL (2007) Ultrahigh molecular weight polyethylene/polypropylene/organo-montmorillonite nanocomposites: phase morphology, rheological, and mechanical properties. *J Appl Polym Sci* 106:3023
30. Liu XH, Wu QJ (2001) PP/clay nanocomposites prepared by grafting-melt intercalation. *Polymer* 42:10013
31. Dragaun H, Hubeny H, Huschik H (1977) Shear-induced  $\beta$ -form crystallization in isotactic polypropylene. *J Polym Sci Part B Polym Phys* 15:1779
32. Samueles RJ (1975) Quantitative structural characterization of the melting behavior of isotactic polypropylene. *J Polym Sci Part B Polym Phys* 13:1417